Biogeosciences

Open Access

EGU

Supplement of

Three decades of simulated global terrestrial carbon fluxes from a data assimilation system confronted with different periods of observations

Karel Castro-Morales et al.

Correspondence to: Karel Castro-Morales (karel.castro.morales@uni-jena.de)
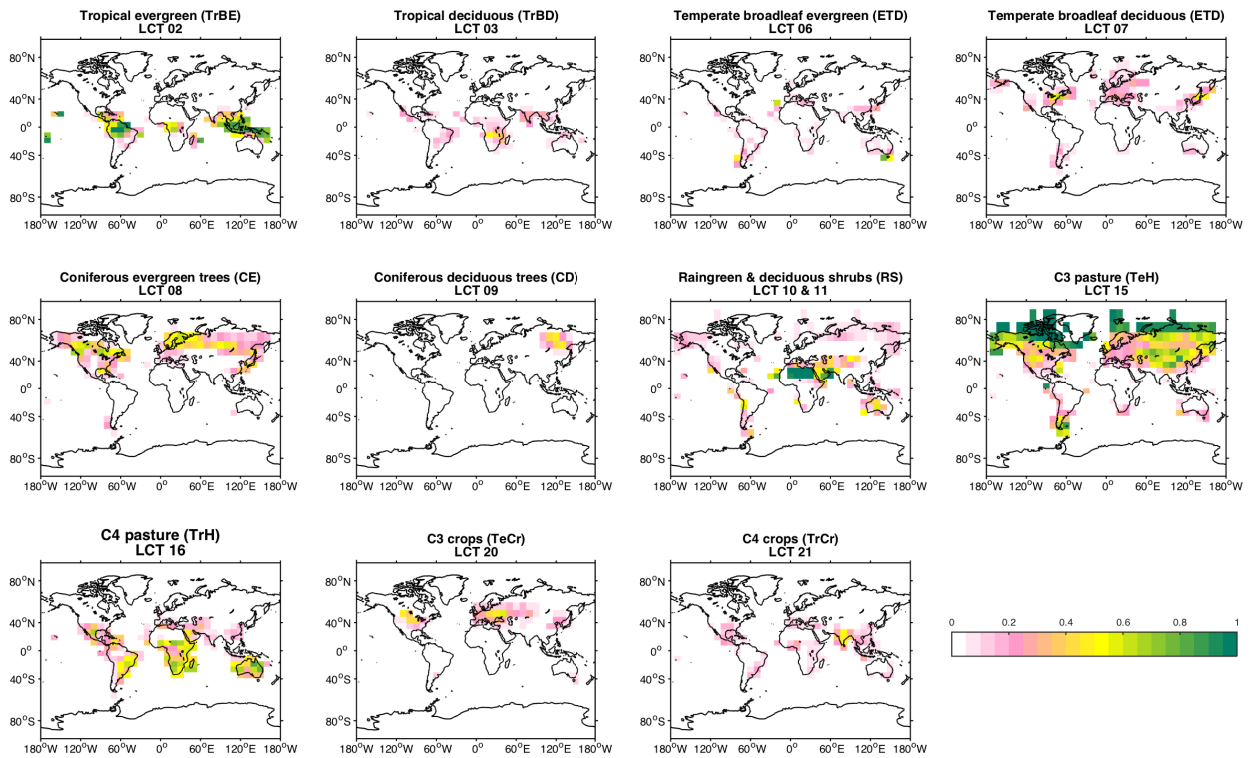
Supplementary material

Figure S1 – Spatial distribution of the fraction on each pixel for the ten plant functional traits prescribed in the model: Tropical evergreen (TrBE) and deciduous (TrBD) trees; Extra-tropical deciduous and evergreen trees (ETD); Coniferous evergreen (CE) and deciduous (CD) trees; Rain-green shrubs (RS); C3 grasses (TeH) and crops (TeCr); C4 grasses (TrH) and crops (TrCr).
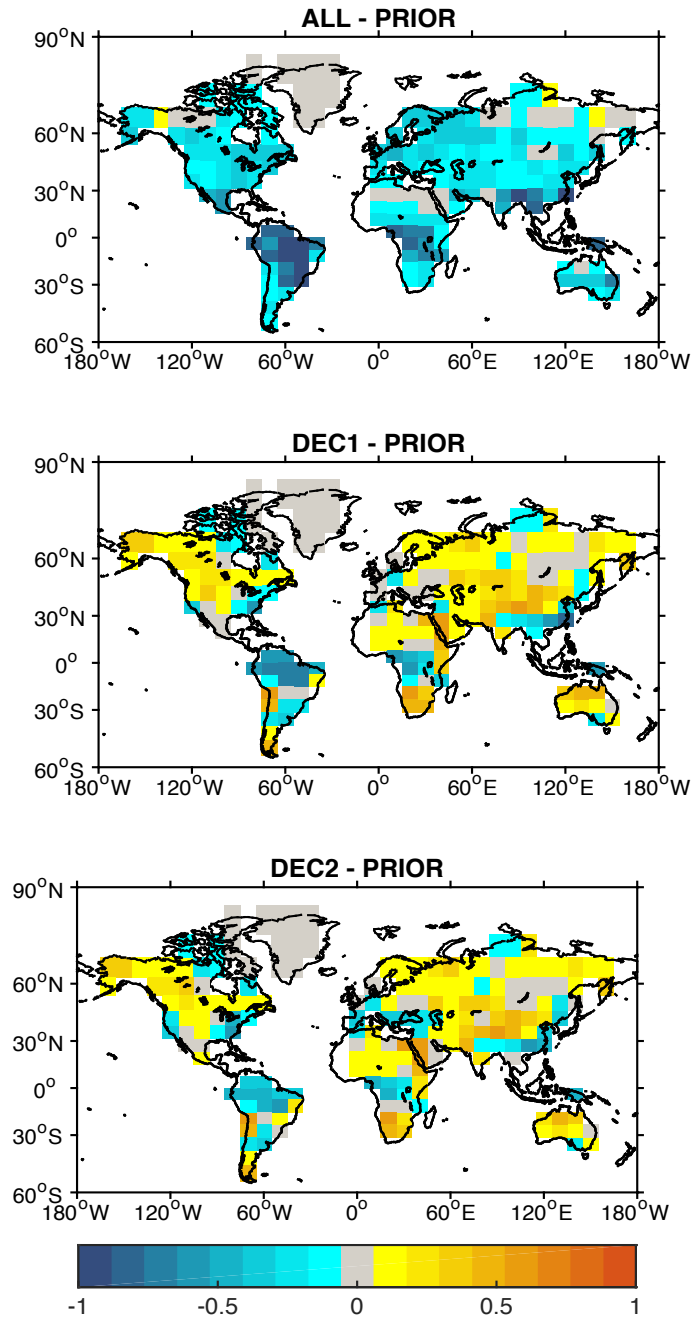
Max LAI [m^2/m^2] (1980-2010)

Figure S2 – Spatial difference between the maximum LAI results from the posterior
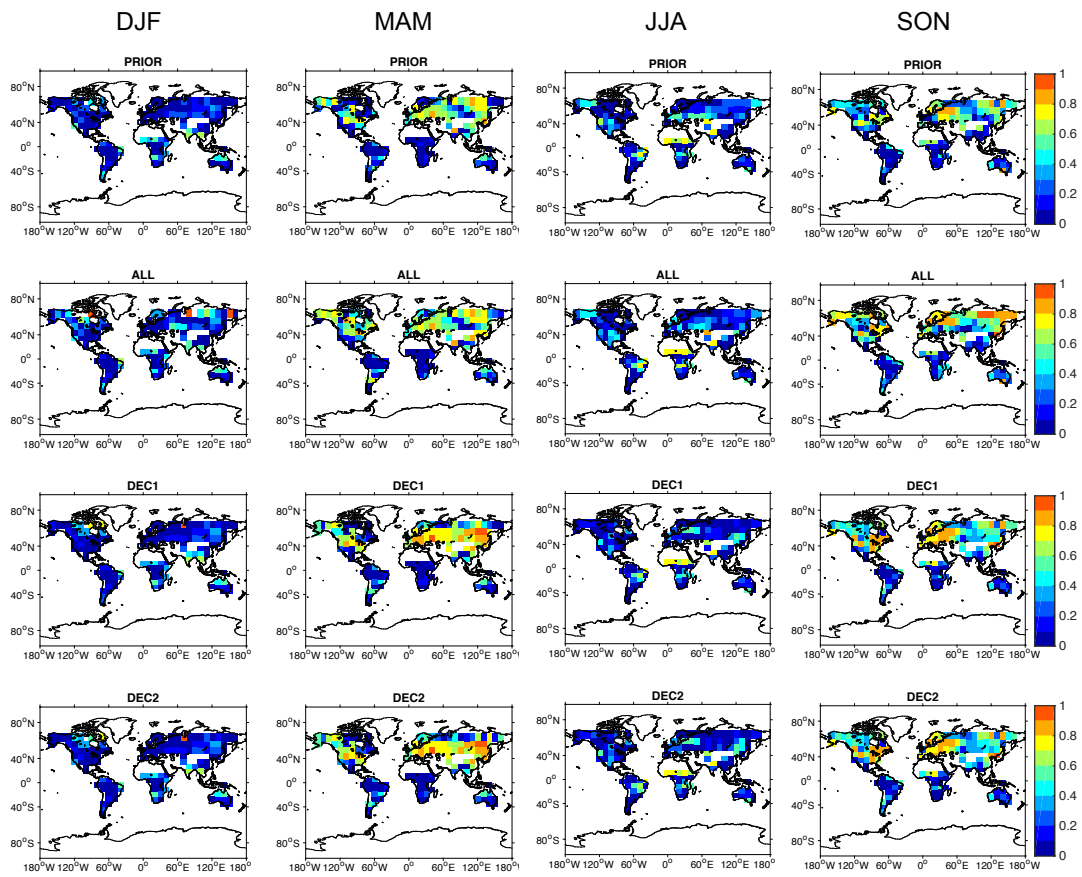and the PRIOR experiments for the total period of the simulation (1980-2010) (LAI).

Figure S3 – Seasonal spatial distribution of R^2 from the correlation between FAPAR from observations and from the model output for the period 1982-2006.
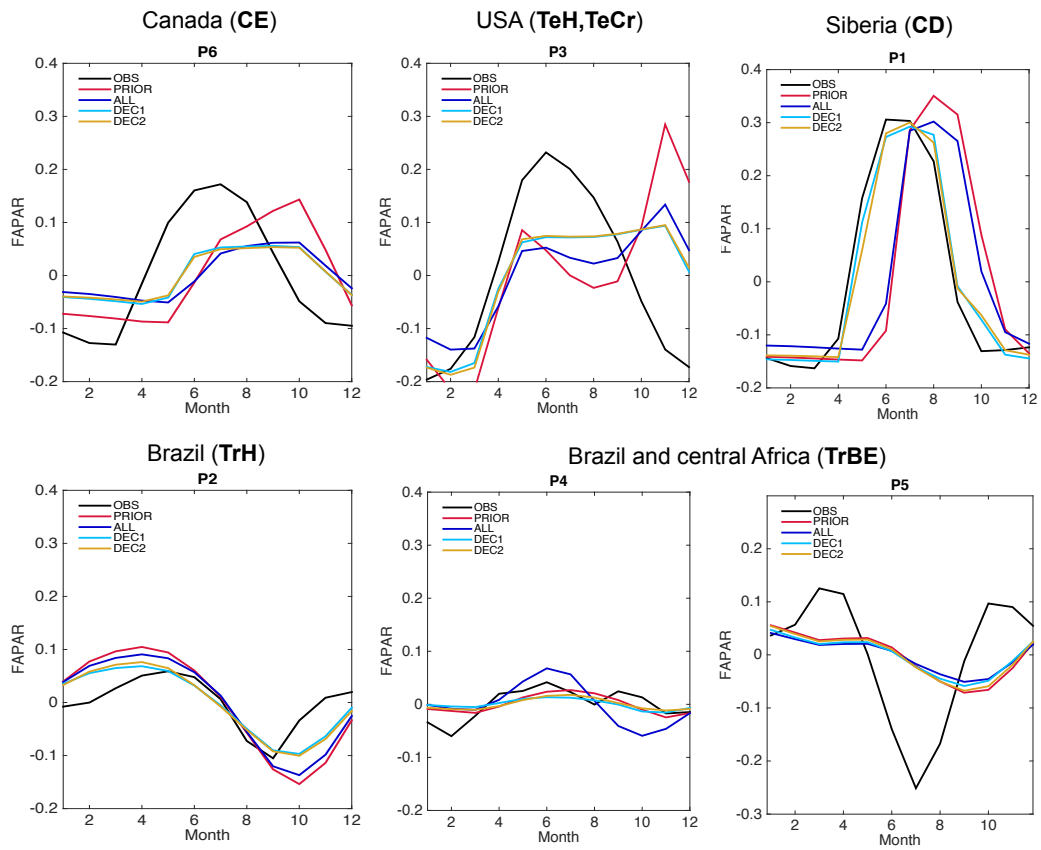
Figure S4 – Mean seasonal cycle of the FAPAR satellite observations and results from the PRIOR and posterior experiments in six globally distributed pixels.
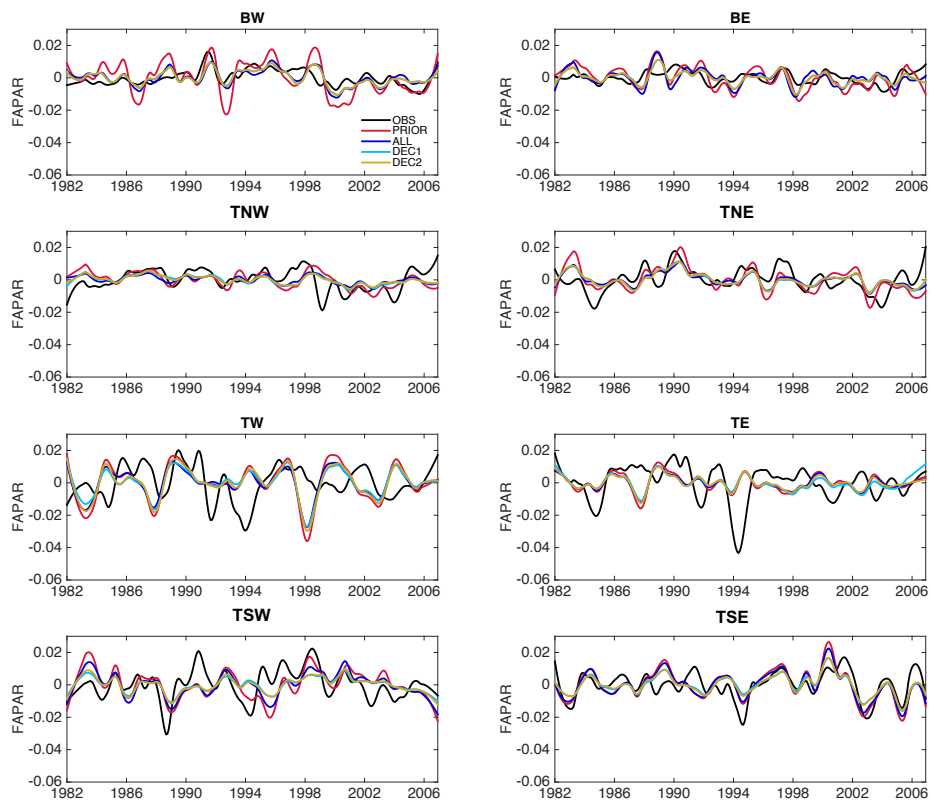
Figure S5 – Interannual variability of FAPAR in the satellite observations and model experiments for the six selected regions.
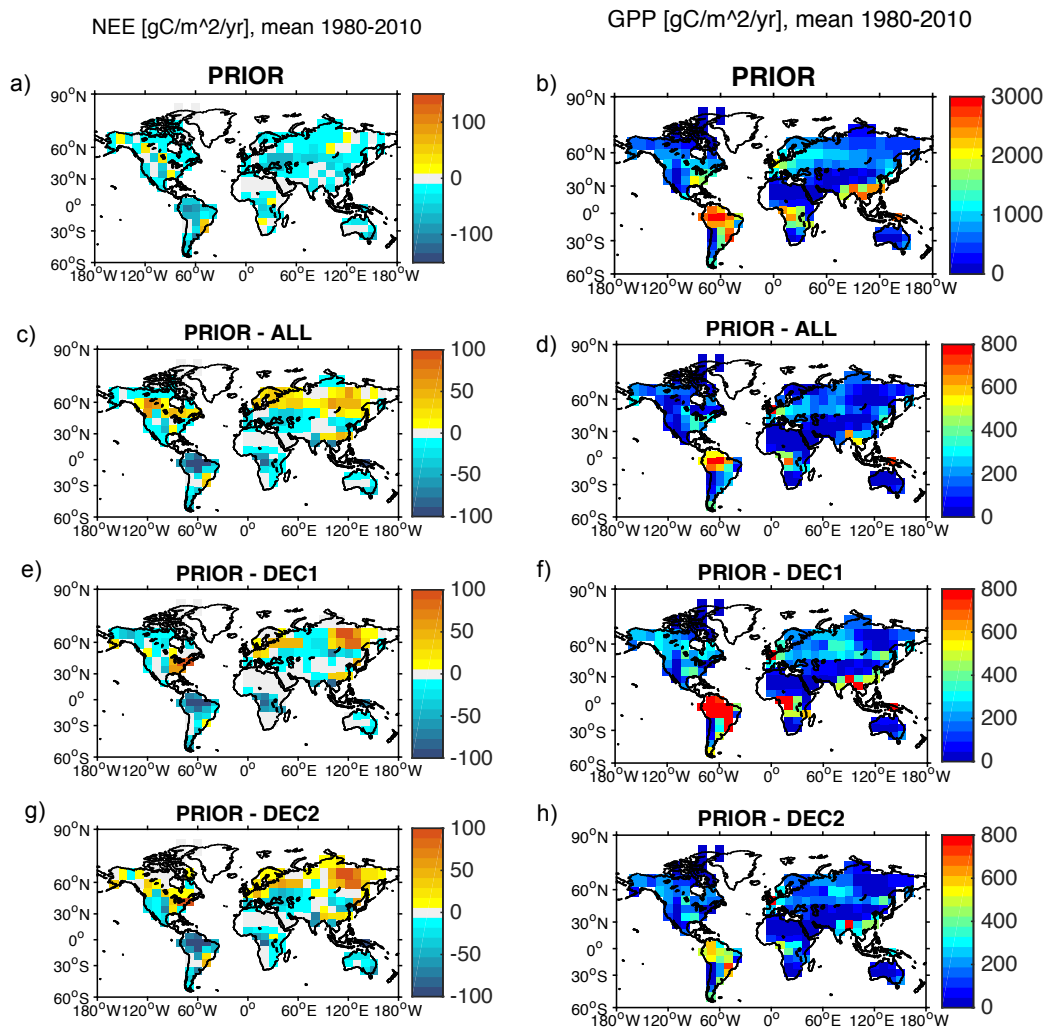
Figure S6 – Spatial distribution of the mean NEE and GPP (both in gC/m^2/yr) for all the period of the simulation (1980-2010) for the PRIOR (a and b) and the difference to the PRIOR for the posterior experiments (c to h).
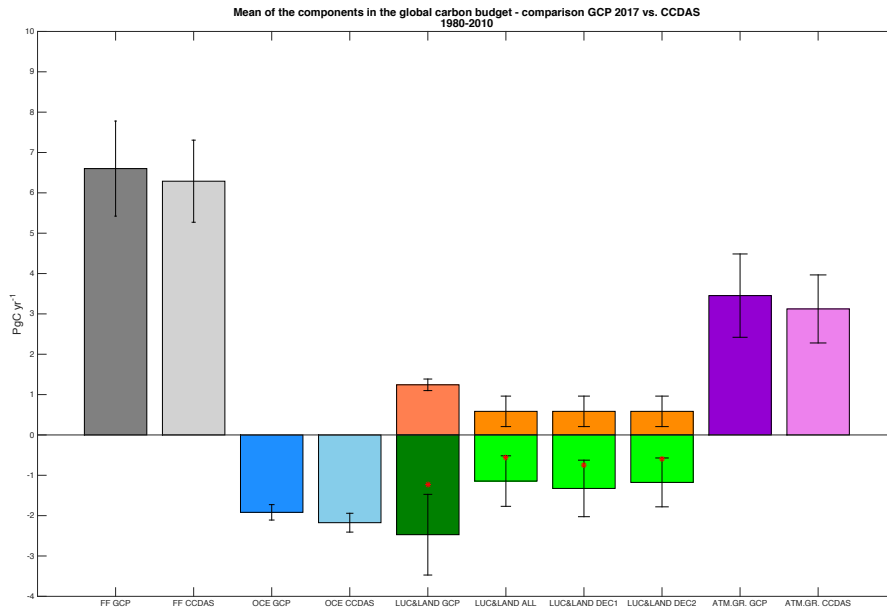
Figure S7 – Mean flux from the C cycle components for the period 1980-2010 from the GCP 2017 and the posterior experiments. Positive is C source to the atmosphere, negative is C sink: Fossil fuels (FF), Ocean (OCE), NEE and flux due to land use change (LUC&LAND) and model calculated atm. CO_2 growth and provided from GCP (ATM.GR.).